IEEE Access
Multidisciplinary | Rapid Review | Open Access Journal

Received September 17, 2020, accepted October 8, 2020, date of publication October 28, 2020, date of current version November 10, 2020.

Digital Object Identifier 10.1109/ACCESS.2020.3034320

Low-Threshold and Tunable Optical Bistability Based on Topological Edge State in One-Dimensional Photonic Crystal Heterostructure With Graphene

YUXIANG PENG[1], JIAO XU[1], SHENPING WANG[1], HU DONG[1], YUANJIANG XIANG[2], XIAOYU DAI[2], JUN GUO[3], SHENGYOU QIAN[1], AND LEYONG JIANG[1]

[1]School of Physics and Electronics, Hunan Normal University, Changsha 410081, China
[2]Institute of Microscale Optoelectronics (IMO), Shenzhen University, Shenzhen 518060, China
[3]Jiangsu Key Laboratory of Advanced Laser Materials and Devices, School of Physics and Electronic Engineering, Jiangsu Normal University, Xuzhou 221116, China

Corresponding authors: Shengyou Qian (qiansy@hunnu.edu.cn) and Leyong Jiang (jiangly28@hunnu.edu.cn)

This work was supported in part by the National Natural Science Foundation of China under Grant 11774088, Grant 11704119, Grant 11874269, and Grant 11704259; in part by the Hunan Provincial Natural Science Foundation of China under Grant 2018JJ3325 and Grant 2018JJ3557; in part by the Guangdong Natural Science Foundation under Grant 2018A030313198; and in part by the Science and Technology Project of Shenzhen under Grant JCYJ20190808143801672, Grant JCYJ20190808150803580, and Grant JCYJ20180305125036005.

ABSTRACT In this article, we present a theoretical analysis of the optical bistability phenomenon of the transmitted light beam in a graphene-based one-dimensional photonic crystal heterostructure in terahertz frequency range. This low-threshold optical bistability originates from the enhancement of the local electric field owing to the excitation of topological edge state at the interface between the two proposed one-dimensional photonic crystals. The results of calculation and simulation show that the hysteretic behavior and the threshold of optical bistability can be adjusted continuously by changing the applied voltage of the graphene. Moreover, the optical bistability of this structure also can be modified by the angle of the incident light and the number of graphene layers. Our findings provide a new method for realizing low threshold and tunable optical bistability in terahertz range, indicating excellent application prospects in the field of all-optical switches and other optical bistable devices.

INDEX TERMS Graphene, low-threshold, optical bistability, topological edge state mode.

I. INTRODUCTION

Optical bistability (OB) is a phenomenon where light is used as a means to control light [1], [2], and two stable output light intensities can be obtained from one input intensity. OB phenomenon provides an effective way for the realization of optical storage [3], information processing [4], phototransistors [5], all-optical switches [6], and other devices. At present, extensive research has being done into the generation and regulation of optical bistability in micro/nanostructures, such as the reports on hyperbolic metamaterials [7], nonlinear magnetoplasmonic nanoparticles [8], spinor polariton condensates [9], and Fabry-Perot cavity [10]. Due to the low nonlinear refractive index of traditional nonlinear optical materials, it is difficult to reduce the incident light power significantly while keeping the OB phenomenon obvious. In this case there is a need for larger size and higher incident light intensity to produce the nonlinear response required by OB in optical bistable devices. But this requirement conflicts with the essence of integrated optics for small size and low power consumption, it is not very practical for high-density integrated circuits and optical paths. In recent years, graphene, as a two-dimensional honeycomb monolayer material with excellent optical and electric qualities, has become the focus of OB research [11]–[13]. Scholars are working on the strong nonlinear effect [14] and tunable conductivity [15] of graphene to realize the generation and regulation of OB phenomenon.

The associate editor coordinating the review of this manuscript and approving it for publication was Bilal Khawaja.

The OB excitation pathway based on graphene has been reported in various structures like graphene-covered nonlinear interfaces [16], dielectric/nonlinear graphene/dielectric heterostructures [17], graphene-wrapped dielectric nanowires [18], etc. At present, reducing the threshold switch power is still the main goal of optical bistable research in optical communication systems. It is feasible to achieve low thresholds in tunable OB devices based on the strong nonlinear effect of special media or the enhanced local field of different nanostructures. For example, there are studies on low threshold OB in graphene/one-dimensional grating structures [19], graphene surface plasmon OB [20], and graphene Tamm plasmon-induced OB [21].

Although the basic principle of OB is very clear, the excitation schemes for low-threshold and simple-structured OB are still challenging work. Recently, the topological edge state mode (TES) in one-dimensional photonic crystal (PhC) has gained in popularity because of its unusual features such as topological protection, backscattering elimination, and local field enhancement [22]. TES modes have been extensively studied in various schemes and structures including the one-dimensional periodic potential and ultra-cold atom system of optical lattices [23], resonant photonic crystals [24], multilayer graphene systems [25] and complex photonic lattices [26]. The expected local field enhancement phenomenon will appear at the interface where TES exists [27]. This means the properties of TES provide a possibility for lowering the threshold of OB. The question arises as to whether we can produce low-threshold tunable OB phenomenon in graphene-based one-dimensional photonic crystals on the basis of TES excitation.

In this article, we study the OB phenomenon of the transmitted and reflected light beams in a one-dimensional photonic crystal heterostructure with graphene, the TES-based OB study on one-dimensional photonic crystal structure with graphene provides a new approach to the research of tunable low-threshold OB and the design of optical bistable devices. The findings can be summarized as follows: (a) in this well-designed structure, the TES mode appears at the interface of photonic crystals and creating positive conditions for lowering the OB threshold; (b) the TES-based threshold value of OB is reduced significantly, and the adjustable conductivity of the graphene can be used to achieve dynamic adjustment of OB.

II. THEORETICAL MODEL AND METHOD

In this heterostructure there are two photonic crystals—PhC1 and PhC2. A layer of graphene is situated at the interface of these two PhCs as shown in Fig. 1. For the convenience of calculation, the photonic crystals are seen as a layered structure; the transmitted and reflected electromagnetic waves in each layer of the medium are marked as F and B; each layer of medium (from left to right) is numbered 1 to 16, and the background material air is numbered 0 and 17, and the black dots are the ellipsis representation of the middle layer. We assume that each layer of the PhC is alternately

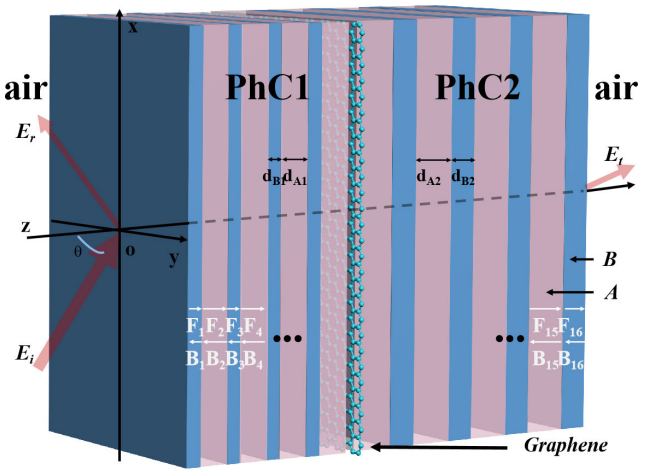

FIGURE 1. Schematic diagram of the proposed TES structure, where the graphene is inserted between two PhCs and the light illuminates from the left to the right at an incidence angle of θ. Here, the period of each PhC is defined as T=4.

superposed by medium A and B, whose thicknesses satisfy $d_{A1} = 270\mu$m,, $d_{A2} = 275\mu$m, and $d_{B2} = 170\mu$m. The period of each PhC is defined as T=4; ε_A and ε_B denote the dielectric constants of medium A and B, respectively. The refractive index is set to be 1.46 for medium A and 2.82 for medium B and the refractive index of A (TPX) is 1.46 and B (TiO_2) is 2.82 [28], [29]. The heterostructure can now be fabricated because the transfer and preparation techniques of PhC and graphene are relatively mature. Besides, since graphene is a two-dimensional material with single-atomic-layer, we consider using electrical conductivity to characterize the graphene. In order to obtain as large a third-order nonlinear conductivity as possible, the incident wave is assumed to be in terahertz band and the external magnetic field is not taken into consideration under random-phase. Then, for the graphene, the isotropic conductivity on its surface would be $\sigma_0 = \sigma_{inter} + \sigma_{intra}$, where σ_{intra} denotes the intra-band conductivity, σ_{inter} denotes the inter-band conductivity. According to the Pauli Exclusion Principle, graphene cannot generate inter-band transition in terahertz band. Therefore, the inter-band conductivity should not be considered [30]:

$$\sigma_0 \approx \frac{ie^2 E_F}{\pi\hbar^2(\omega + i/\tau)}, \tag{1}$$

In this equation, e is the electric charge and ω is the angular frequency of the incident light; E_F stands for the Fermi energy, τ represents the relaxation time of the graphene, $\hbar$ refers to the reduced Planck's constant, and $E_F = \hbar\sqrt{\pi n_{2D}}$ (n_{2D} is the carrier density). Then, we can use the following equation to express the three-order nonlinear conductivity coefficient of the graphene without regard to two photon coefficients [31]:

$$\sigma_3 = -\frac{9ie^4 v_F^2}{8\pi\hbar^2 E_F \omega^3} \tag{2}$$

where v_F denotes the Fermi velocity of electrons and $v_F \approx 10^6$m/s. It can be seen from (1) and (2) that both the linear

and nonlinear conductivity coefficients are susceptible to the Fermi energy of graphene. This provides us a feasible way of flexibly regulating optical bistable devices with graphene.

In this article, we assume that the graphene is parallel to the x-axis and the electromagnetic field propagation is in the direction of z-axis. The graphene is located at z=0. Then, we can use $\sigma = \sigma_0 + \sigma_3 \left|E_{8y}(z=0)\right|^2$ to describe the conductivity of the graphene. If we only consider the case of TE polarization, the electromagnetic field of the incident air layer would be:

$$\begin{cases} E_{0y} = E_i e^{ik_{0z}[z+4(d_{A1}+d_{B1})]} e^{ik_x x} \\ +E_r e^{-ik_{0z}[z+4(d_{A1}+d_{B1})]} e^{ik_x x} \\ H_{0x} = -\dfrac{k_{0z}}{\mu_0 \omega} E_i e^{ik_{0z}[z+4(d_{A1}+d_{B1})]} e^{ik_x x} \\ +\dfrac{k_{0z}}{\mu_0 \omega} E_r e^{-ik_{0z}[z+4(d_{A1}+d_{B1})]} e^{ik_x x} \\ H_{0z} = \dfrac{k_x}{\mu_0 \omega} E_i e^{ik_{0z}[z+4(d_{A1}+d_{B1})]} e^{ik_x x} \\ +\dfrac{k_x}{\mu_0 \omega} E_r e^{-ik_{0z}[z+4(d_{A1}+d_{B1})]} e^{ik_x x} \end{cases} . \quad (3)$$

The electromagnetic field of the transmitted air layer would be:

$$\begin{cases} E_{17y} = E_t e^{ik_{0z}[z-4(d_{A2}+d_{B2})]} e^{ik_x x} \\ H_{17x} = -\dfrac{k_{0z}}{\mu_0 \omega} E_t e^{ik_{0z}[z-4(d_{A2}+d_{B2})]} e^{ik_x x} \\ H_{17z} = \dfrac{k_x}{\mu_0 \omega} E_t e^{ik_{0z}[z-4(d_{A2}+d_{B2})]} e^{ik_x x} \end{cases} , \quad (4)$$

where E_i is he amplitude of the incident electric field, E_r is that of the reflected electric field, and E_t is that of the transmitted electric field; k_0 is the wave vector in vacuum; ε_0 and μ_0 are the permittivity and magnetic conductivity of the free space. Thus, the following equation is constructed to express the electric field and magnetic field of each medium layer in PhC:

$$\begin{cases} E_{\Pi y} = F_\Pi e^{ik_{\zeta z}[z+(nd_{Ag}+md_{Bg})]} e^{ik_x x} \\ +B_\Pi e^{-ik_{\zeta z}[z+(nd_{Ag}+md_{Bg})]} e^{ik_x x} \\ H_{\Pi x} = -\dfrac{k_{\zeta z}}{\mu_0 \omega} F_\Pi e^{ik_{\zeta z}[z+(nd_{Ag}+md_{Bg})]} e^{ik_x x} \\ +\dfrac{k_{\zeta z}}{\mu_0 \omega} B_\Pi e^{-ik_{\zeta z}[z+(nd_{Ag}+md_{Bg})]} e^{ik_x x} \\ H_{\Pi z} = \dfrac{k_x}{\mu_0 \omega} F_\Pi e^{ik_{\zeta z}[z+(nd_{Ag}+md_{Bg})]} e^{ik_x x} \\ +\dfrac{k_x}{\mu_0 \omega} B_\Pi e^{-ik_{\zeta z}[z+(nd_{Ag}+md_{Bg})]} e^{ik_x x} \end{cases} , \quad (5)$$

where $\prod = \{1, 2, 3 \ldots 16\}$, $\zeta = A, B$, $g =$ PhC1, PhC2, and $n, m = \{0, 1, 2, 3, 4\}$. $k_0 = \omega/c$, $k_x = k_0\sqrt{\varepsilon_0}\sin\theta$, and $k_{\zeta z} = \sqrt{k_0^2 \varepsilon_\zeta - k_x^2}$; θ is the incident angle. As a precondition for this research, the electromagnetic fields on both sides of the graphene should be continuous, then we can build the following equation according to the boundary conditions at the interface between two adjacent media where z=0.

$$\begin{cases} E_{9y}(0) = E_{8y}(0) \\ H_{8x}(0) - H_{9x}(0) = \sigma E_{8y}(0) \end{cases} \quad (6)$$

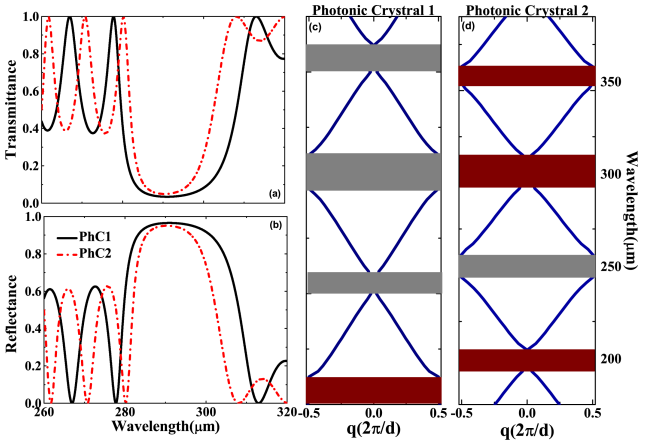

FIGURE 2. (a) The transmittance spectra and (b) reflectance spectra of individual PhC1 (black solid line) and PhC2 (red dot-dashed line); the band structure of (c) PhC1 and (d) PhC2; each gray band indicates a bandgap with a positive topological phase, while the brown ones indicate those with negative topological phases.

Finally, after calculating with the above formula, the OB phenomenon can be obtained.

III. RESULTS AND DISCUSSIONS

The relationships of the incident wavelength to the transmittance and reflectance of PhC1 and PhC2 are shown in Fig. 2(a) and 2(b), respectively. The bandgap width of PhC1 near the 300μm wavelength is greater than that of PhC2, which is consistent with the band diagram at 1 THz in Fig. 2(c) and 2(d). It can be seen from Fig. 2(c) and 2(d) that there are four gaps in the 0.6-1.3THz frequency range, the q represents the normalized frequency. It is noteworthy that the bandgaps near 1 THz are classified as broad bandgaps that present varied topological features. Therefore, it is possible to obtain TES at the interface between PhC1 and PhC2 by adding up the ZaK phases near 1THz [32]. In other words, the TES effect is excited at the interface between PhC1 and PhC2, and the local field enhancement, as shown in Fig. 3(c), is generated [29].

Based on the transfer matrix, we draw the transmittance spectrum, reflectance spectrum, and the electric-field distribution of the composite photonic crystal structure, as shown in Fig. 3(a), Fig. 3(b), and Fig. 3(c), respectively. The period of the proposed structure is 4, which helps us to control the peak of TES at the 1THz band. After amplifying the transmittance peak and reflectivity dip of the structure, it is found that the fitting curves conform with typical Lorentzian lines. This means there is Lorentz resonance at the interface of the PhC heterostructure [33]. In contrast, the peak values of the transmittance and reflectance of the whole composite structure are reduced with the introduction of graphene, indicating the possibility for the emergence and regulation of OB owing to the strong nonlinear effect and adjustable characteristics of graphene. Fig. 3(c) shows the electric field distribution. Obviously, the electric field is significantly enhanced at the interface of the photonic crystal heterostructure, and an unusual optical phenomenon appears, thus proving the existence of TES.

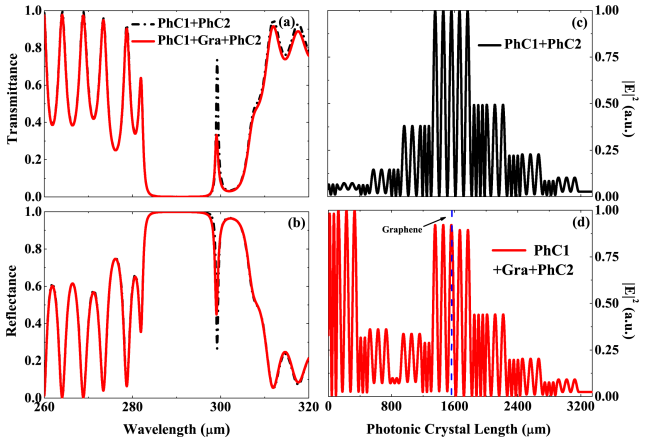

FIGURE 3. (a) The transmittance spectra and (b) reflectance spectra of the "PhC1+PhC2" heterostructure (black dot-dashed line) and "PhC1+ graphene +PhC2" (red solid line) heterostructure; the calculated electric field of (c) the PhC heterostructure and (d) the PhC heterostructure with graphene.

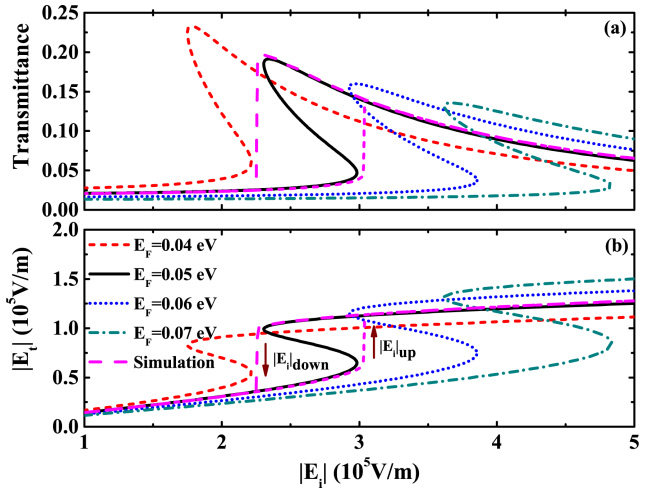

FIGURE 4. Dependence of (a) the transmittance and (b) transmitted electric field on the incident electric field for different Fermi energy E_F of graphene. The pink dashed line shows the calculation results of COMSOL Multiphysics. Here, $\lambda = 300\mu$m, $\tau = 0.6$ps, $\theta = 0^o$.

Next, we discuss the OB phenomenon in graphene-based one-dimensional photonic crystals on the basis of TES excitation, which changes with the incident electric field under different parameters. It can be seen from (2) that the third-order nonlinear conductivity is relatively strong on the basis of the 1THz frequency range. At the same time, the local field enhancement at the PhC interface is obtained by TES. This leads to an increase of E in the graphene conductivity formula $\sigma = \sigma_0 + \sigma_3 |E|^2$, which in turn strengthens its nonlinear part. In simple terms, we can excite the OB phenomenon with an extremely low-threshold through the graphene-based one-dimensional PhC heterostructure by TES. After introducing the concept of TES, we found that the threshold of OB under TES effect is several magnitude orders lower than the threshold excited by other structures [21].

As shown in Fig. 4(a), we have also calculated the relationship between the transmittance and incident electric field under different levels of graphene Fermi energy. As the Fermi energy increases, the upper and lower thresholds (i.e. $|E_i|_{up}$ and $|E_i|_{down}$) rise, and so does the threshold width. The OB threshold also increases with the graphene Fermi energy, while the transmittance of the graphene-based PhC heterostructure continues to decrease. We can assume PhC1 and PhC2 as two Bragg mirrors, then, combine (1) and (2), the two conductivity formulas of the graphene, to obtain the scattering matrix expression of the entire structure [34], [35]:

$$M_{\text{phc1}} = \frac{1}{t_{\text{phc1}}}\begin{bmatrix} -1 & -|r_{\text{phc1}}| \\ |r_{\text{phc1}}| & 1 \end{bmatrix} \tag{7}$$

$$M_{\text{phc2}} = \frac{1}{t_{\text{phc2}}}\begin{bmatrix} -1 & -|r_{\text{phc2}}| \\ |r_{\text{phc2}}| & 1 \end{bmatrix},$$

$$M = M_{\text{phc1}} \cdot M_{\text{graphene}} \cdot M_{\text{phc2}}, \tag{8}$$

where t and r are the transmission and reflection amplitudes of the photonic crystal, respectively, and $|t|^2 + |r|^2 = 1$. We can use transmission coefficients to express the correlation of the incident electric field with the transmitted electric field:

$$\frac{E_t}{E_i} = t = \frac{1}{|M_{11}|} = \frac{t_{\text{phc1}} t_{\text{phc2}}}{\left|\zeta\left[1-|r_{\text{phc1}}|\,|r_{\text{phc2}}|-(|r_{\text{phc1}}|+|r_{\text{phc2}}|)\right]-(r_{\text{phc2}})^2+1\right|}, \tag{9}$$

where $\zeta = \mu_0 c(\sigma_0 + \sigma_3 |E_t|^2)/2$. Here, E_t, the transmitted electric fied, is assumed to be a purely real number, and $Y = |E_i|^2$, $X = |E_t|^2$, then we get:

$$Y = X\,|\Gamma(X)|^2,$$

$$\Gamma = \frac{[\mu_0 c(\sigma_0 + \sigma_3 X)]\left[1 - |r_{phc1}| \cdot |r_{phc2}|\right]}{2t_{phc1} \cdot t_{phc2}}$$

where

$$-\frac{[\mu_0 c(\sigma_0 + \sigma_3 X)]\,(|r_{phc1}| + |r_{phc2}|)}{2t_{phc1} \cdot t_{phc2}} - \frac{|r_{phc2}|^2 + 1}{2t_{phc1} \cdot t_{phc2}}. \tag{10}$$

According to (10), the incident electric field is largely a multivalued function of the transmitted electric field. The condition required for the existence of OB is that the discriminant Δ of the derivative function of (10) must be greater than zero, so that there is one Y value corresponding to three X values:

$$\Delta = \frac{(\text{Rc}\mu_0\sigma_3)^2\left(|r_2|^2-1\right)^2}{(t_1 t_2)^4} + \frac{\left[6Rc\mu_0\sigma_0 - 4R^3\sigma_0\sigma_3^2(c\mu_0)^3\right]\left(|r_2|^2-1\right)}{(t_1 t_2)^4} - \frac{\left(\frac{\mu_0 c}{2}\right)^2 R^4\,(\sigma_0\sigma_3)^2\,(8\mu_0 c - 24)}{(t_1 t_2)^4},$$

$$R = 1 - |r_1|\,|r_2| - |r_1| - |r_2|\,. \tag{11}$$

From the calculation we know $\Delta > 0$ and the two zeros of the derivative function would satisfy:

$$X_{ext,1} \approx -\frac{\sigma_0}{3\sigma_3}\; X_{ext,2} \approx -\frac{\sigma_0}{\sigma_3}. \tag{12}$$

Combined it with (10) to transform $\Delta Y = Y_{ext,1} - Y_{ext,2}$ into:

$$\Delta Y = \left(\frac{176}{243}Z - \frac{64}{27}\right)\left(\frac{\left(eV_f\right)^2 e^4\omega^3}{(\pi\hbar)^2(\omega + 1/\tau)^3 (t_1 t_2)^2}\right) E_f^4, \quad (13)$$

where ΔY is the absolute value of the difference between the upper and lower thresholds of OB. Fig. 4(b) shows the multivalued curve between the transmitted and the incident electric field. Whenthe Fermi energy in graphene's nonlinear conductivity increases from 0.04 eV to 0.07 eV, the OB threshold increases rapidly, and the hysteresis loop width also rises significantly. When graphene increases to a large value, the transmittance of incident wave decreases sharply, indicating that the large Fermi energy of graphene has considerable loss for the transmission of incident wave, which may not be conducive to the realization of low-threshold optical bistable devices in the 1THz band. It can be seen from the changing regularity in Fig. 4(a) and Fig. 4(b) that the transmittance jumps from about 0.02 to 0.18 with the increase of the incident electric field. In comparison, the transmitted electric field shifts from 0.35×10^5V/m to 1.02×10^5V/m at a Fermi energy level of 0.05 eV, which is about 45% of the incident electric field. And as the Fermi energy rises, there is a gradual increase in the transmitted electric field despite the decline of the transmittance, indicating the enhancement of local field at the interface of the PhC structure by TES and the resultant increase in the transmitted electric field. It can be seen from Fig. 4 that the low threshold of OB phenomenon can be stimulated from the TES. Unlike photonic crystal with magneto-optical layer [36], the structure is different, the transmittance and reflectance are different, and the mechanism used to achieve low threshold is different. The pink dashed line in Fig. 4 shows the calculation results of COMSOL Multiphysics. The curve plotted at a Fermi energy level of 0.05 eV is taken as reference; the finite element (FEM) method is applied to check the linear and nonlinear response effects of the proposed structure, and the rigorous coupled-wave theory is adopted to verify the accuracy of the numerical results. In the FEM method, the setting of structural parameters is consistent with the mathematical calculation. According to the figures, the results of COMSOL multi-physics calculation are consistent with the transfer matrix method, which reflects the correctness of the conclusions of this article. It is shown that the TES effect is susceptible to the Fermi energy of graphene, which could help in controlling the threshold value of OB by merely adjusting the Fermi energy. Therefore, it provides an effective method for controlling OB by the applied voltage. Meanwhile, it plays a very active role in reducing OB thresholds.

In addition, we found that OB is also subject to the relaxation time (τ) of the graphene. As shown in Fig. 5(a), the optical hysteresis loop and width have a tendency to increase with the relaxation time, resulting in a gradual decrease of the OB threshold. When the relaxation time (τ) satisfies $\tau = 0.5$ps, the hysteresis width would be $\Delta|E_i| = |E_i|_{up} - |E_i|_{down} = 0.52 \times 10^5$V/m; when the relaxation time

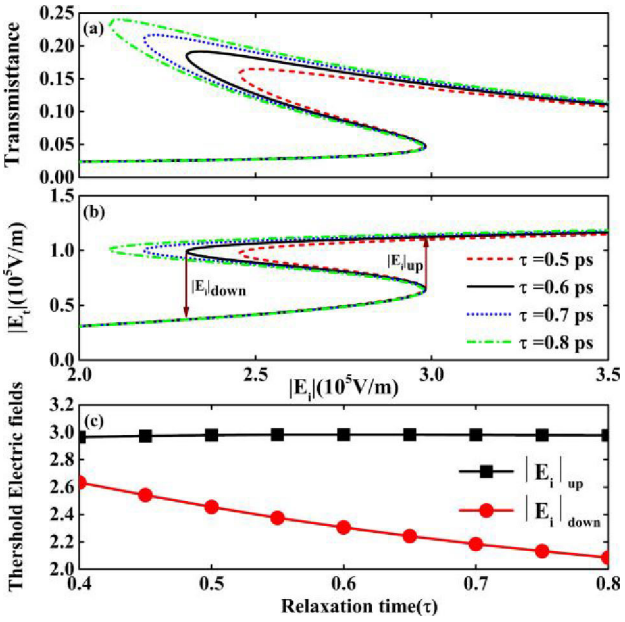

FIGURE 5. Dependence of (a) the transmittance and (b) transmitted electric field on the incident electric field for different relaxation time τ of graphene. (c) Dependence of $|E_i|_{down}$ and $|E_i|_{up}$ on different relaxation time τ of graphene. Here, $\lambda = 300\mu$m, $E_F = 0.05$ eV, $\theta = 0^o$.

fulfills $\tau = 0.8$ps, the hysteresis width would be $\Delta|E_i| = 0.89 \times 10^5$V/m. Overall, the OB threshold is reduced by 0.37×10^5V/m, and the hysteresis width is widened by nearly 1.7 times. Besides, the hysteresis curve will disappear and the OB will not exist if the relaxation time is small enough that $|E_i|_{up}$ and $|E_i|_{down}$ tend to superpose with each other. Compared with the OB excited by traditional micro/nano metal devices, the OB excited by the proposed structure on the basis of TES effect has flexible thresholds and controllable hysteresis width. The dynamically tunable characteristics of graphene provide another feasible way for the fabrication and design of optical bistable devices.

The OB is influenced not only by the graphene parameters in (13) but also by the angle of incident light and the number of graphene layers (see Fig. 6). With other parameters remain unchanged, the hysteresis width and the threshold value of OB continue to rise when the incident angle increases from $\theta = 0^o$ to $\theta = 6^o$. As shown in Fig. 6(a), the OB phenomenon still exists in the transmitted electric field when the incident angle has been reduced to $\theta = 0^o$. This is mainly because the TES excited by the vertical incidence of light in the proposed PhC structure could enhance the local field enhancement and create the necessary conditions for the appearance of low-threshold OB. Since the thickness of single-layer graphene is very thin (only 0.34nm), its electrical conductivity can be approximated by $\sigma \approx N\sigma_0$(N $\leq$ 6) [37], [38]. The hysteresis width is about $\Delta|E_i| = 0.68 \times 10^5$V/m when the number of graphene layers is N=1, and the hysteresis width is about $\Delta|E_i| = 4.29 \times 10^5$V/m at N=4 in Fig. 6(b). It can be concluded that the threshold and hysteresis width of OB increase simultaneously with the number of graphene layers. The above results have proved that it is possible to control OB

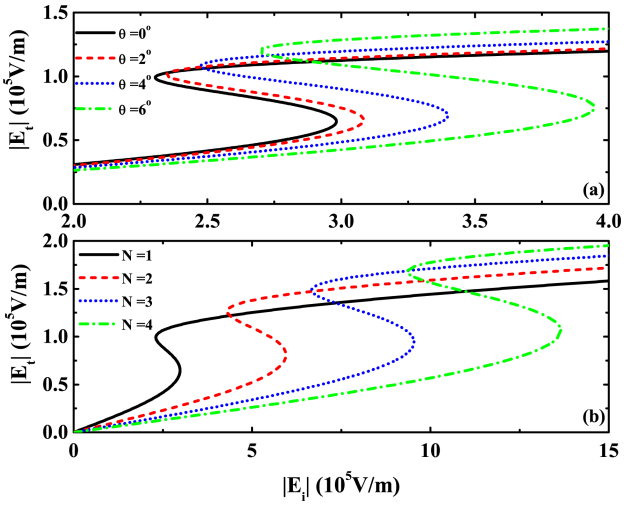

FIGURE 6. Dependence of (a) the angle of incident light θ and (b) number of graphene layers N for the transmitted electric field on the incident electric field. Here, $\lambda = 300\mu$m, $E_F = 0.05$ eV, $\tau = 0.6$ps.

by adjusting the incident angle and the number of graphene layers.

Finally, the graphene-based one-dimensional photonic crystal heterostructure can also calculate the low threshold OB phenomenon of the reflected light beam in terahertz frequency range. The behavioral regulation mechanism of graphene for reflected OB phenomenon is similar to the above. Conclusively, the tunable nonlinear conductivity of graphene is also a deciding factor in the realization of low threshold reflective OB.

IV. CONCLUSION

In summary, we have theoretically studied the OB phenomenon in graphene-based one-dimensional photonic crystals on the basis of TES excitation at terahertz band. The results show that the TES has a positive effect of reducing the threshold value of OB. The excitation of TES can significantly increase the intensity of the local electric field in the proposed structure, and finally realize the low threshold OB phenomenon by enhancing the third-order nonlinear conductivity of the graphene. Meanwhile, through further calculations, we know that the hysteresis width, as well as the upper and lower thresholds of the OB phenomenon, is flexibly regulated by the graphene conductivity and closely related to the number of graphene layers and the incident angle of the light. Finally, the correctness of the mathematical calculation results is further verified by numerical simulations. The structure proposed in this article is simple, easy to prepare, novel mechanism and tunable. We have every reason to believe that the TES-based low-threshold tunable OB in the proposed one-dimensional photonic crystal structure with graphene has practical applications and excellent potential for innovating new all-optical switches.

REFERENCES

[1] H. M. Gibbs, *Optical Bistability: Controlling Light With Light*. Orlando, FL, USA: Academic, 1985.

[2] E. Abraham, "Optical bistability and related devices," *Rep. Prog. Phys.*, vol. 45, no. 8, p. 815, 1982, doi: 10.1088/0034-4885/45/8/001.

[3] J. Sakaguchi, "All-optical memory operation of 980-nm polarization bistable VCSEL for 20-Gb/s PRBS RZ and 40-Gb/s NRZ data signals," *Opt. Express*, vol. 18, no. 12, pp. 12362–12370, May 2010, doi: 10.1364/OE.18.012362.

[4] K. Inoue and M. Yoshino, "Bistability and waveform reshaping in a DFB-LD with side-mode light injection," *IEEE Photon. Technol. Lett.*, vol. 7, no. 2, pp. 164–166, Feb. 1995, doi: 10.1109/68.345910.

[5] M. F. Yanik, "All-optical transistor action with bistable switching in a photonic crystal cross-waveguide geometry," *Opt. Lett.*, vol. 28, no. 24, pp. 2506–2508, Dec. 2003, doi: 10.1364/OL.28.002506.

[6] A. Hurtado, "Optical bistability and nonlinear gain in 1.55 μm VCSOA," *Electron. Lett.*, vol. 42, no. 8, pp. 483–484, Apr.2006, doi: 10.1049/el:.20060478.

[7] M. Kim, "Optical bistability based on hyperbolic metamaterials," *Opt. Express*, vol. 26, no. 9, pp. 11620–11632, Apr. 2018, doi: 10.1364/OE.26.011620.

[8] W. Yu, "Optical tristability and ultrafast Fano switching in nonlinear magnetoplasmonic nanoparticles," *Phys. Rev. B, Condens. Matter*, vol. 97, no. 7, p. 075436, Feb. 2018, doi: 10.1103/PhysRevB.97.075436.

[9] L. Pickup, "Optical bistability under nonresonant excitation in spinor polariton condensates," *Phys. Rev. Let.*, vol. 120, no. 22, May 2018, Art. no. 225301, doi: 10.1103/PhysRevLett.120.225301.

[10] A. Grieco, "Optical bistability in a silicon waveguide distributed Bragg reflector Fabry–Perot resonator," *J. Lightwave. Technol.*, vol. 30, no. 14, pp. 2352–2355, Jul. 2012, doi: 10.1109/JLT.2012.2197731.

[11] A. K. Geim and K. S. Novoselov, "The rise of graphene," *Nature Mater.*, vol. 6, no. 3, pp. 183–191, Mar. 2007, doi: 10.1038/nmat1849.

[12] A. H. Castro Neto, F. Guinea, N. M. R. Peres, K. S. Novoselov, and A. K. Geim, "The electronic properties of graphene," *Rev. Modern Phys.*, vol. 81, no. 1, pp. 109–162, Jan. 2009, doi: 10.1103/RevModPhys.81.109.

[13] K. S. Novoselov, V. I. Fal, L. Colombo, P. R. Gellert, M. G. Schwab, and K. Kim, "A roadmap for graphene," *Nature*, vol. 490, no. 7419, pp. 192–200, Oct. 2012, doi: 10.1038/nature11458.

[14] H. Zhang, "Z-scan measurement of the nonlinear refractive index of graphene," *Opt. Lett.*, vol. 37, no. 11, pp. 1856–1858, Jun. 2012, doi: 10.1364/OL.37.001856.

[15] Z. Q. Li, E. A. Henriksen, Z. Jiang, Z. Hao, M. C. Martin, P. Kim, H. L. Stormer, and D. N. Basov, "Dirac charge dynamics in graphene by infrared spectroscopy," *Nature Phys.*, vol. 4, no. 7, p. 532, Jun. 2008, doi: 10.1038/nphys989.

[16] Y. Xiang, X. Dai, J. Guo, S. Wen, and D. Tang, "Tunable optical bistability at the graphene-covered nonlinear interface," *Appl. Phys. Lett.*, vol. 104, no. 5, Feb. 2014, Art. no. 051108, doi: 10.1063/1.4863927.

[17] X. Dai, "Tunable optical bistability of dielectric/nonlinear graphene/dielectric heterostructures," *Opt. Express*, vol. 23, no. 5, pp. 6497–6508, Mar. 2015, doi: 10.1364/OE.23.006497.

[18] K. Zhang, "Optical bistability in graphene-wrapped dielectric nanowires," *Opt. Express*, vol. 25, no. 12, pp. 13747–13759, Jun. 2017, doi: 10.1364/OE.25.013747.

[19] J. Guo, L. Jiang, Y. Jia, X. Dai, Y. Xiang, and D. Fan, "Low threshold optical bistability in one-dimensional gratings based on graphene plasmonics," *Opt. Express*, vol. 25, no. 6, pp. 5972–5981, Mar. 2017, doi: 10.1364/OE.25.005972.

[20] X. Dai, L. Jiang, and Y. Xiang, "Low threshold optical bistability at terahertz frequencies with graphene surface plasmons," *Sci. Rep.*, vol. 5, no. 1, pp. 1–11, Jul. 2015, doi: 10.1038/srep12271.

[21] L. Jiang, "Graphene Tamm plasmon-induced low-threshold optical bistability at terahertz frequencies," *Opt. Mater. Express*, vol. 9, no. 1, pp. 139–150, Jan. 2019, doi: 10.1364/OME.9.000139.

[22] C. Li, "Unidirectional transmission in 1D nonlinear photonic crystal based on topological phase reversal by optical nonlinearity," *AIP. Adv.*, vol. 7, Feb. 2017, Art. no. 025203, doi: 10.1063/1.4976013.

[23] M. Atala, M. Aidelsburger, J. T. Barreiro, D. Abanin, T. Kitagawa, E. Demler, and I. Bloch, "Direct measurement of the Zak phase in topological Bloch bands," *Nature Phys.*, vol. 9, no. 12, pp. 795–800, Nov. 2013, doi: 10.1038/nphys2790.

[24] A. V. Poshakinskiy, A. N. Poddubny, L. Pilozzi, and E. L. Ivchenko, "Radiative topological states in resonant photonic crystals," *Phys. Rev. Lett.*, vol. 112, no. 10, pp. 1–5, Mar. 2014, doi: 10.1103/PhysRevLett.112.107403.

[25] L. Ge, L. Wang, M. Xiao, W. Wen, C. T. Chan, and D. Han, "Topological edge modes in multilayer graphene systems," *Opt. Express*, vol. 23, no. 17, pp. 21585–21595, 2015, doi: 10.1364/OE.23.021585.
[26] H. Schomerus, "Topologically protected midgap states in complex photonic lattices," *Opt. Lett.*, vol. 38, no. 11, pp. 1912–1914, Jun. 2013, doi: 10.1364/OL.38.001912.
[27] W. Gao, "Fano-resonance in one-dimensional topological photonic crystal heterostructure," *Opt. Express*, vol. 26, no. 7, pp. 8634–8644, Mar. 2018, doi: 10.1364/OE.26.008634.
[28] L. Jiang, "Manipulating the optical bistability at terahertz frequency in the Fabry–Perot cavity with graphene," *Opt. Express*, vol. 23, no. 24, pp. 31181–31191, Nov. 2015, doi: 10.1364/OE.23.031181.
[29] D. R. Lide, *Handbook of Chemistry and Physics*, 76th ed., Boca Raton, FL, USA: CRC Press, 1995.
[30] Y. V. Bludov, A. Ferreira, N. M. R. Peres, and M. I. Vasilevskiy, "A primer on surface plasmon-polaritons in graphene," *Int. J. Modern Phys. B*, vol. 27, no. 10, Apr. 2013, Art. no. 1341001, doi: 10.1142/S0217979213410014.
[31] N. M. R. Peres, Y. V. Bludov, J. E. Santos, A.-P. Jauho, and M. I. Vasilevskiy, "Optical bistability of graphene in the terahertz range," *Phys. Rev. B, Condens. Matter*, vol. 90, no. 12, Sep. 2014, Art. no. 125425, doi: 10.1103/physrevb.90.125425.
[32] M. Xiao, Z. Q. Zhang, and C. T. Chan, "Surface impedance and bulk band geometric phases in one-dimensional systems," *Phys. Rev. X*, vol. 4, no. 2, Apr. 2014, Art. no. 021017, doi: 10.1103/PhysRevX.4.021017.
[33] J. D. Joannopoulos, *Photonic Crystals: Molding the Flow of Light*. Princeton, NJ, USA: Princeton Univ. Press, 1995.
[34] A. Ferreira, N. M. R. Peres, R. M. Ribeiro, and T. Stauber, "Graphene-based photodetector with two cavities," *Phys. Rev. B, Condens. Matter*, vol. 85, no. 11, Mar. 2012, Art. no. 115438, doi: 10.1103/PhysRevB.85.115438.
[35] T. Zhan, X. Shi, Y. Dai, X. Liu, and J. Zi, "Transfer matrix method for optics in graphene layers," *J. Phys., Condens. Matter*, vol. 25, no. 21, May 2013, Art. no. 215301, doi: 10.1088/0953-8984/25/21/215301.
[36] A. G. Ardakani, "Highly tunable bistability using an external magnetic field in photonic crystals containing graphene and magnetooptical layers," *J. Appl. Physi.*, vol. 121, no. 2, pp. 1–7, Jan. 2017, doi: 10.1063/1.4972306.
[37] C. Casiraghi, A. Hartschuh, E. Lidorikis, H. Qian, H. Harutyunyan, T. Gokus, K. S. Novoselov, and A. C. Ferrari, "Rayleigh imaging of graphene and graphene layers," *Nano Lett.*, vol. 7, no. 9, pp. 2711–2717, Sep. 2007, doi: 10.1021/nl071168m.
[38] H. Yan, X. Li, B. Chandra, G. Tulevski, Y. Wu, M. Freitag, W. Zhu, P. Avouris, and F. Xia, "Tunable infrared plasmonic devices using graphene/insulator stacks," *Nature Nanotechnol.*, vol. 7, no. 5, pp. 330–334, Apr. 2012, doi: 10.1038/nnano.2012.59.

YUXIANG PENG received the B.S. and M.S. degrees from the Central South University of Forestry and Technology, China, in 2015 and 2018, respectively. He is currently pursuing the Ph.D. degree in physics with Hunan Normal University, Changsha, China. His current research interests include nonlinear optics, photonic crystals, micro/nano optoelectronic devices, and photonic devices.

JIAO XU received the B.S. degree in measurement and control technology and instrument from Xiangtan University, China. She is currently pursuing the master's degree in electronic science and technology with Hunan Normal University, Changsha, China. Her current research interests include micro/nano optoelectronic devices, photonic crystals, nonlinear optics, and photonic devices.

SHENPING WANG received the B.S. degree in electronic information engineering from Changsha University, China. She is currently pursuing the degree in electronic science and technology with Hunan Normal University, Changsha, China. Her current research interest includes micro nano optoelectronic devices and applications.

HU DONG received the B.S. degree in electronic science and technology from the Hunan University of Arts and Sciences, China, in 2005, and the M.S. degree from the School of Physics and Electronics, Hunan Normal University, China, in 2008, where he is currently pursuing the Ph.D. degree. Since 2017, he has been an Associate Professor with the School of Information Science and Engineering, Changsha Normal University. His current research interests include biomedical electronics and signal processing.

YUANJIANG XIANG received the M.S. degree in physics and microelectronics sciences and the Ph.D. degree in computer application technology from Hunan University, China, in 2006 and 2011, respectively. From 2008 to 2009, he was engaged as a Visiting Scholar with the Department of Electronic Engineering, Purdue University. From 2012 to 2014, he was engaged as a Postdoctoral Researcher with the School of Electrical and Electronic Engineering, Nanyang Technological University, Singapore. He is currently a Professor with Hunan University. His main research interest includes the transmission and control of light and electromagnetic waves. In recent years, advanced research results have been obtained in the research of new nonlinear optical effects and topological optics.

XIAOYU DAI received the B.S. degree in electric engineering from Chongqing University, Chongqing, China, in 2002, and the Ph.D. degree in computer application technology from Hunan University, Changsha, China, in 2009. She is currently an Associate Professor with Shenzhen University, Shenzhen, China. Her main research interests include the theory of nonlinear metamaterials, graphene, and the interaction of light with 2-D materials and Dirac materials.

JUN GUO received the B.Sc. degree in communication engineering and the Ph.D. degree in circuits and systems from Hunan University, in 2010 and 2015, respectively. He has worked as a Project Officer in EEE with Nanyang Technological University, from October 2013 to October 2014. He has worked as a Postdoctoral Researcher with Shenzhen University from September 2015 to December 2017. He has been working with the School of Physics and Electronic Engineering, Jiangsu Normal University. His research interests include nonlinear optics and plasmonics.

SHENGYOU QIAN received the Ph.D. degree from Shanghai Jiaotong University (SJTU), China, in 1997. He joined the faculty at Hunan Normal University, in 1997, where he is currently a Professor with the School of Physics and Electronics. His current research interests include optoelectronics, ultrasonic electronics, sensor technology, and signal processing.

LEYONG JIANG received the B.S. degree in electronic information science and technology from Hunan Normal University, Changsha, China, in 2006, and the Ph.D. degree in computer application technology from Hunan University, China, in 2014. From 2014 to 2016, he was engaged as a Postdoctoral Researcher with Shenzhen University. Since 2016, he has been an Associate Professor with the School of Physics and Electronics, Hunan Normal University. His current research interests include micro/nano optoelectronic devices, metamaterials, photonic crystals, nonlinear optics, and photonic devices.